

Theoretical study of quasiparticle states near the surface of a quasi-one-dimensional organic superconductor $(\text{TMTSF})_2\text{PF}_6$

Y. Tanuma

Department of Applied Physics, Nagoya University, Nagoya 464-8063, Japan

K. Kuroki

Department of Applied Physics and Chemistry, The University of Electro-Communications, 1-5-1 Chofugaoka, Chofu-shi, Tokyo 182-8585, Japan

Y. Tanaka

Department of Applied Physics, Nagoya University, Nagoya 464-8063, Japan

S. Kashiwaya

Electrotechnical Laboratory, 1-1-4 Umezono, Tsukuba, 305-0045, Japan

(December 2, 2024)

Quasiparticle states near the surface of an quasi-one-dimensional organic superconductor $(\text{TMTSF})_2\text{PF}_6$ is studied based on an extended Hubbard model on a quasi-one dimensional lattice at quarter-filling. Three types of pairing symmetries, (i) p -wave, (ii) d -wave, or (iii) f -wave are assumed. The resulting surface density of states has characteristic features for each pairing symmetry: i) a zero-energy peak (ZEP) in a U-shaped structure, ii) a V-shaped structure without ZEP, and iii) a ZEP in a V-shaped structure. From these results, we propose that the the tunneling spectroscopy serves as a strong method to identify the the pairing symmetry in $(\text{TMTSF})_2\text{PF}_6$.

PACS numbers: 74.70.Kn, 74.50.+r, 73.20.-r

In recent years, pairing symmetry in various unconventional superconductors, such as the high- T_c cuprates, heavy fermion systems, Sr_2RuO_4 , organic superconductors, and so on, has been extensively studied both experimentally and theoretically.^{1–3} In particular, quasi-one-dimensional (Q1D) organic superconductors $(\text{TMTSF})_2\text{X}$ ($\text{X}=\text{PF}_6^-$, ClO_4^- , etc.) have recently attracted much attention as a possible *spin-triplet* superconductor. Experimentally, the observation of a large critical magnetic field H_{c2} exceeding Pauli paramagnetic limit⁵, as well as an unchanged Knight shift across T_c ,⁶ strongly suggest spin-triplet pairing. As for the orbital part of the pair wave function, the presence of nodes in the pair potential on the Fermi surface has been suggested from NMR measurements for $(\text{TMTSF})_2\text{ClO}_4$ ⁷ and $(\text{TMTSF})_2\text{PF}_6$,⁶ which exhibit the absence of Hebel-Slichter peak as well as a power-law decay of T_1^{-1} below T_c . On the other hand, a thermal conductivity measurement has suggested the absence of nodes on the Fermi surface in $(\text{TMTSF})_2\text{ClO}_4$.⁸

Theoretically, several previous studies have proposed a triplet p -wave pairing state,^{9–11} for which the nodes of the pair potential do not intersect the Fermi surface. On the other hand, a spin-singlet d -wave-like pairing mediated by spin fluctuations has been proposed by several authors.^{13–15} This is because superconductivity lies right next to the $2k_F$ spin density wave (SDW) phase in the pressure-temperature phase diagram.¹² Moreover, one of the present authors have recently proposed¹⁸ that triplet f -wave-like pairing may dominate over d - and p -wave in $(\text{TMTSF})_2\text{PF}_6$ due to a combination of

Q1D Fermi surface, coexistence of $2k_F$ SDW and $2k_F$ charge density wave (CDW) suggested from diffuse X-ray scattering,^{16,17} and an anisotropy in the spin fluctuations.

Thus, the situation is not settled either experimentally or theoretically. The purpose of the present study is to propose an experimental method to determine which one of the pairing symmetries is realized in $(\text{TMTSF})_2\text{PF}_6$.

Now, for the high- T_c cuprates, which has a singlet d -wave pair potential, it has been clarified that the internal phase causes a drastic interference effect in the quasiparticle states near surfaces or interfaces, enabling us to detect the sign change in the pair potential. Namely, a zero-energy bound state (ZES) at a (110) surface of a d -wave superconductor reflects the sign-change of the effective pair potential in the process of the reflection of quasiparticle at the surface¹⁹. The formation of ZES results in a peak in the surface density of states (SDOS) at the Fermi energy (zero-energy) and manifests itself as a so-called zero-bias conductance peak (ZBCP) observed in scanning tunneling spectroscopy,^{20–24} which is considered as a strong evidence for a sign change in the pair potential.

Recently, Sengupta *et al.* have proposed that the pairing symmetry in $(\text{TMTSF})_2\text{X}$ ²⁵ can be determined from the presence/absence of the ZES on the surface. Although their study points out an important aspect, they consider a purely one-dimensional system in the actual calculation, and their argument is mainly restricted to the absence/presence of ZEP, from which the p -wave and f -wave pairings cannot be distinguished. In fact, as we

shall see, one has to look into the overall line shape of the SDOS to distinguish p - and f -wave pairings. Since the detailed line shape of the SDOS is significantly influenced by the actual shape of the Fermi surface, we have to consider a more realistic lattice structure, in which the quasi one-dimensionality (warping) of the Fermi surface is taken into account.

In order to meet this requirement, we consider an extended Hubbard model on a Q1D lattice at quarter-filling, extending the previous study on a 2D square lattice.²⁶ We concentrate on $(\text{TMTSF})_2\text{PF}_6$ because there is no complexity (unit cell doubling) due to anion ordering like in $(\text{TMTSF})_2\text{ClO}_4$.²⁷ Three types of physically plausible pairings (i) triplet ' p -wave' (ii) singlet ' d -wave' and (iii) triplet ' f -wave' are studied. The spatial dependence of the pair potentials is determined self-consistently, and the SDOS is calculated using the self-consistently determined pair potentials. We propose from the calculation results that the quasiparticle tunneling spectroscopy should serve as a strong method to identify the pairing symmetry in $(\text{TMTSF})_2\text{PF}_6$.

The extended Hubbard model is given as

$$\begin{aligned} \mathcal{H} = & - \sum_{\langle \mathbf{i}, \mathbf{j} \rangle_a, \alpha} \left(t_a c_{\mathbf{i}, \alpha}^\dagger c_{\mathbf{j}, \alpha} + \text{H.c.} \right) \\ & - \sum_{\langle \mathbf{i}, \mathbf{j} \rangle_b, \alpha} \left(t_b c_{\mathbf{i}, \alpha}^\dagger c_{\mathbf{j}, \alpha} + \text{H.c.} \right) \\ & - \frac{V}{2} \sum_{\langle \mathbf{i}, \mathbf{j} \rangle_m, \alpha, \beta} c_{\mathbf{i}, \alpha}^\dagger c_{\mathbf{j}, \beta}^\dagger c_{\mathbf{j}, \beta} c_{\mathbf{i}, \alpha} - \mu \sum_{\mathbf{i}, \alpha} c_{\mathbf{i}, \alpha}^\dagger c_{\mathbf{i}, \alpha}, \quad (1) \end{aligned}$$

where $c_{\mathbf{i}, \alpha}$ [$c_{\mathbf{i}, \alpha}^\dagger$] is the annihilation [creation] operator of an electron with spin $\alpha = \uparrow, \downarrow$ at site $\mathbf{i} = (i_a, i_b)$. Here t_a [t_b] is the hopping integral, and $\langle \mathbf{i}, \mathbf{j} \rangle_a$ [b] stands for summation over nearest neighbor pairs in the a [b]-axis direction, respectively. V is the inter-electron potential between sites separated by m lattice spacings in the a -direction, and $\langle \mathbf{i}, \mathbf{j} \rangle_m$ represents summation over pairs of sites separated by m lattice spacings. m depends on the choice of the pairing considered. We choose $t_b/t_a = 0.1$ in order to take into account the Q1D Fermi surface of $(\text{TMTSF})_2\text{PF}_6$, which is open in the k_b -direction. The chemical potential μ is determined so that the band is quarter-filled.

By applying a mean-field approximation, $\Delta_{\mathbf{i}, \mathbf{j}}^{\alpha, \beta} = \frac{V}{2} \langle c_{\mathbf{i}, \alpha} c_{\mathbf{j}, \beta} \rangle$ is introduced, which represents the superconducting pair potential for pairs formed by α -spin electron on the \mathbf{i} th site and β -spin electron on the \mathbf{j} th site. We assume that $\Delta_{\mathbf{i}, \mathbf{j}}^{\alpha, \beta}$ is proportional to δ_{i_b, j_b} , where i_b and j_b are coordinates in the b -direction. Thus the unit cell contains N_L sites in the a -direction and one site in the b -direction. We consider three pairing symmetries shown in Fig. 1. Namely, (i) p -wave: $S_b = 0$ (S_b is the b -component of the total spin of a pair) triplet pairing between sites separated by 2 lattice spacings ($m_p = 2$). This is a p -wave pairing because the pair potential has a $2\Delta_p \sin 2k_a a$, k -dependence in the bulk state, so that

the pair potential changes its sign as $+-$ along the Fermi surface (see Fig. 1). (ii) d -wave: singlet pairing between sites separated by 2 lattice spacings ($m_d = 2$). This is a ' d -wave' pairing in the sense that the pair potential changes its sign as $+-+-$ along the Fermi surface due to a its $2\Delta_d \cos 2k_a a$ k -dependence in the bulk state. (iii) f -wave: $S_b = \pm 1$ triplet pairing between sites separated by 4 lattice spacings ($m_f = 4$). This is an ' f -wave' pairing in the sense that the pair potential changes its sign as $+-+-+-$ along the Fermi surface due to its $2\Delta_f \sin 4k_a a$ k -dependence in the bulk state. These three pairings are physically plausible in the sense that they are consistent with the spin alignment of the $2k_F$ SDW phase of a quarter filled ($k_F = \frac{\pi}{4a}$) system with an easy axis in the b -direction.¹⁸ In other words, the $2k_F$ spin fluctuations can favor pairing in these channels.

In order to represent $\Delta_{\mathbf{i}, \mathbf{j}}^{\alpha, \beta}$ in a more convenient way, we introduce a new coordinate j along the a -direction. The original coordinate \mathbf{j} is represented as $\mathbf{j} = (j, j_b)$ with $j = 1, \dots, N_L$. In the b -direction, we assume N_b unit cells, and the electrons are Fourier transformed as $C_{j\alpha}(k_b) = \sum_{j_b=1}^{N_b} c_{j\alpha} e^{-ik_b j_b a}$, and $C_{j\beta}(-k_b) = \sum_{j_b=1}^{N_b} c_{j\beta} e^{ik_b j_b a}$, where $-\pi/a < k_b \leq \pi/a$, $k_b = \frac{2\pi}{N_b} n$ with n being an integer.

FIG. 1. (a) An illustration of Cooper pairing in real space and (b) the shape of Fermi surface for $t_b/t_a = 0.1$ at quarter-filling and the pair potential for (i) triplet ' p -wave' ($m_p = 2$), (ii) singlet ' d -wave' ($m_d = 2$), and (iii) triplet ' f -wave' ($m_f = 4$). In (a), the pairs are depicted by dashed lines, and in (b) $+$ ($-$) denotes the region where the sign of the pair potential is positive (negative).

After the Fourier transformation, the mean-field Hamiltonian becomes

$$\begin{aligned} \mathcal{H}_{\text{MF}} = & \sum_{k_b, i, j} \left[\begin{array}{cccc} C_{i\uparrow}^\dagger(k_b) & C_{i\downarrow}^\dagger(k_b) & C_{i\uparrow}(-k_b) & C_{i\downarrow}(-k_b) \end{array} \right] \\ & \times \left[\begin{array}{cccc} H_{ij}(k_b) & 0 & \Delta_{ij}^{\uparrow\uparrow} & \Delta_{ij}^{\uparrow\downarrow} \\ 0 & H_{ij}(k_b) & \Delta_{ij}^{\downarrow\uparrow} & \Delta_{ij}^{\downarrow\downarrow} \\ \Delta_{ji}^{*\uparrow\uparrow} & \Delta_{ji}^{*\uparrow\downarrow} & -H_{ji}(-k_b) & 0 \\ \Delta_{ji}^{*\downarrow\uparrow} & \Delta_{ji}^{*\downarrow\downarrow} & 0 & -H_{ji}(-k_b) \end{array} \right] \end{aligned}$$

$$\times \begin{bmatrix} C_{j\uparrow}(k_b) \\ C_{j\downarrow}(k_b) \\ C_{j\uparrow}^\dagger(-k_b) \\ C_{j\downarrow}^\dagger(-k_b) \end{bmatrix}, \quad (2)$$

$$H_{ij}(k_b) = - \sum_{\pm} [t_a \delta_{i,j\pm 1} + 2t_b \cos(k_b a) \delta_{i,j} - \mu \delta_{i,j}]. \quad (3)$$

Here, for simplicity, the off diagonal part in Eq.(2) is assumed in the following forms. For the p -wave state,

$$\Delta_{ij}^{\uparrow\downarrow} = \Delta_{ij}^{\downarrow\uparrow} = \sum_{\pm} \Delta_{ij}^p \delta_{i,j\pm 2}, \quad \Delta_{ij}^{\uparrow\uparrow} = \Delta_{ij}^{\downarrow\downarrow} = 0, \quad (4)$$

for the d -wave state,

$$\Delta_{ij}^{\uparrow\downarrow} = -\Delta_{ij}^{\downarrow\uparrow} = \sum_{\pm} \Delta_{ij}^d \delta_{i,j\pm 2}, \quad \Delta_{ij}^{\uparrow\uparrow} = \Delta_{ij}^{\downarrow\downarrow} = 0, \quad (5)$$

and for the f -wave state,

$$\Delta_{ij}^{\uparrow\uparrow} = \Delta_{ij}^{\downarrow\downarrow} = \sum_{\pm} \Delta_{ij}^f \delta_{i,j\pm 4}, \quad \Delta_{ij}^{\uparrow\downarrow} = \Delta_{ij}^{\downarrow\uparrow} = 0. \quad (6)$$

We have taken the total number of sites as $N_L = 500$ and $N_b = 50$. The value of the pair potential and the chemical potential in the bulk with $V/t_a = 4.0$ are (i) $\Delta_p/t_a = 0.280$, $\mu/t_a = 1.39$, (ii) $\Delta_d/t_a = 0.164$, $\mu/t_a = 1.39$, and (iii) $\Delta_f/t_a = 0.244$, $\mu/t_a = 1.38$, respectively.

In the actual numerical calculation, the above Hamiltonian \mathcal{H}_{MF} is diagonalized by Bogoliubov transformation²⁸ given by $C_{i\alpha}(k_b) = \sum_{\nu} \mathcal{U}_{i,\nu} \gamma_{\nu}(k_b)$, and $C_{j\beta}(-k_b) = \sum_{\nu} \gamma_{\nu}^\dagger(k_b) \mathcal{U}_{N_L+j,\nu}^*$, where ν is the index which specifies the eigenstates. Then, the mean-field Hamiltonian described in Eq. (2) is rewritten as $\mathcal{H}_{\text{MF}} = \sum_{k_b,\nu} E_{\nu}(k_b) \gamma_{\nu}^\dagger(k_b) \gamma_{\nu}(k_b)$, where the operator $\gamma_{\nu}(k_b)$ satisfies the fermion's anticommutation relation. The spatial dependence of the pair potential with l -wave pairing symmetry is determined self-consistently as

$$\Delta_{j,j\pm m_l}^l = \frac{V}{2} \sum_{k_b,\nu} \mathcal{U}_{j\pm m_l,\nu} \mathcal{U}_{N_L+j,\nu}^* \{1 - f[E_{\nu}(k_b)]\}, \quad (7)$$

where $f[E_{\nu}(k_b)]$ denotes the Fermi distribution function. The procedure is iterated until the pair potential Δ_{ij}^l is obtained fully self-consistently. We calculate the SDOS using the pair potential determined self-consistently. In order to compare our theory with scanning tunneling microscopy (STM) experiments, we assume that the STM tip is metallic with a flat density of states (DOS), and that the tunneling probability is finite only for the nearest site from the tip. This assumption has been verified through the study of tunneling conductance of unconventional superconductors. This is because the magnitude of the tunneling probability of an electron is sufficiently low in the actual STM experiments. The resulting tunneling conductance spectrum converges to the normalized SDOS³

$$\bar{\rho}(E) = \frac{\int_{-\infty}^{\infty} d\omega \rho_{1,S}(\omega) \text{sech}^2(\frac{\omega - E}{2k_B T})}{\int_{-\infty}^{\infty} d\omega \rho_N(\omega) \text{sech}^2(\frac{\omega + 2\Delta_l}{2k_B T})} \quad (8)$$

$$\rho_{1,S}(\omega) = 2 \sum_{k_b} \sum_{\nu} |\mathcal{U}_{1,\nu}|^2 \delta\{\omega - E_{\nu}(k_b)\}. \quad (9)$$

at low temperatures, where $\rho_{i,S}(\omega)$ denotes the SDOS at the i -th site from the surface in the superconducting state and $\rho_N(\omega)$ denotes the DOS in the normal state. In this paper, $\rho_N(\omega)$ is obtained from the DOS at the $N_L/2$ -th site far away from the surface.

FIG. 2. The left panels are the spatial dependences of the pair potentials along the a -axis near the surface in the l -wave state ($l = p, d, f$), and the right panels show the SDOS at the surface normal to the a - or b -axis along with the bulk density of states.

The obtained spatial dependences of the p -, d -, and f -wave pair potentials and the corresponding SDOS are plotted in Fig. 2. Since the spatial dependence of the pair potential is complex, we define the following quantities given by

$$\begin{aligned} \Delta_{j,\pm x}^p &\equiv \text{Re}[\Delta_{j,j\pm 2}^p]/\Delta_p, & \text{Im}[\Delta_{j,j\pm 2}^p] &= 0, \\ \Delta_{j,\pm x}^d &\equiv \text{Re}[\Delta_{j,j\pm 2}^d]/\Delta_d, & \text{Im}[\Delta_{j,j\pm 2}^d] &= 0, \\ \Delta_{j,\pm x}^f &\equiv \text{Im}[\Delta_{j,j\pm 4}^f]/\Delta_f, & \text{Re}[\Delta_{j,j\pm 4}^f] &= 0. \end{aligned} \quad (10)$$

to visualize the spatial dependences clearly. The left panels of Fig. 2 is the obtained result for the spatial dependence of the pair potential near a surface normal to the *a*-axis, and the right panels show the SDOS at the surface normal to the *a*- or the *b*-axis along with the bulk DOS.

First, let us look into the results for the triplet *p*-wave pairing state shown in the upper panels of Fig. 2 [see Fig. 2(a) and 2(b)]. Since triplet Cooper pair is formed between two electrons with 2 lattice spacings, $\Delta_{j,x}^p = -\Delta_{j+2,-x}^p$ is satisfied. Both the magnitude of $\Delta_{j,x}^p$ and $\Delta_{j,-x}^p$ is suppressed near the surface and approaches 1 and -1 in the middle of superconductor, respectively. As shown in Fig. 2(b), the corresponding DOS has a U-shaped gap structure similar to that of the conventional *s*-wave pairing due to the fact that the nodes of the pair potential do not intersect the Fermi surface. The ZEP shows up in SDOS at the surface normal to *a*-axis due to the formation of ZES, since an injected and reflected quasiparticle feel different sign of the pair potential³⁰. On the other hand, at the surface normal to the *b*-axis, since an injected and reflected quasiparticle feel the same pair potential, the ZES is not formed and the resulting SDOS has no ZEP, resulting in a overall line shape similar to that of the bulk DOS. These results for the *p*-wave pairing are consistent with those in Ref. 25.

Next, we look into the corresponding quantities in singlet *d*-wave pairing case [see Fig. 2(c) and 2(d)]. Since the pair is formed between sites separated by 2 lattice spacings, $\Delta_{j,x}^d = \Delta_{j+2,-x}^d$ is satisfied. The obtained spatial dependence of the pair potential exhibits a atomic-scale spatial oscillation near the surface and converges to the bulk value toward the middle of the lattice. These features are similar to the previous results for the extended Hubbard model on a 2D square lattice²⁶. The corresponding SDOS (and bulk DOS) has a V-shaped structure due to the existence of nodes of the pair potential on the Fermi surface. However, since an injected and reflected quasiparticle feel the same pair potential both at the surfaces normal to *a*- and *b*-axis, no ZEP appears at the SDOS [see Fig. 2(d)]. Due to the absence of the pair potential along the *b*-axis, the ZEP never appears for arbitrary orientation of the surface which is strikingly different from the case of the high- T_c cuprates²⁰.

Finally, we move on to the case of the triplet *f*-wave pairing. The *f*-wave pair [see Fig. 1(a) (iii)] is formed between sites separated by 4 lattice spacings, so the resulting pair potential satisfies $\Delta_{j,x}^f = -\Delta_{j+4,-x}^f$. As seen from Fig. 2(e), the obtained pair potential has a complex spatial dependence as compared to that of the *p*-wave pairing. Comparing Fig. 2(b) and Fig. 2(f), it can be seen that the *f*-wave pairing belongs to the same class as that of the *p*-wave pairing *as far as the absence/presence of the ZEP is concerned*, as has been pointed out in Ref. 25. However, since the *f*-wave pair potential has nodes on the Fermi surface, the resulting SDOS (and bulk DOS) has a V-shaped structure similar to that for the *d*-wave case

in sharp contrast with the case of *p*-wave pairing.

In total, as summarized in Table I, the *p*-, *d*-, and *f*-wave pairings can be clearly distinguished from the combination of the overall line shape of the SDOS and the presence/absence of the *a*-axis ZEP.

In summary, we have studied the quasiparticle SDOS of an organic superconductor $(\text{TMTSF})_2\text{PF}_6$ based on an extended Hubbard model on a Q1D lattice at quarter filling. The non-local feature of the pair potential and the atomic-scale geometry of the surface are explicitly taken into account in the present calculation. Three types of pairing symmetries, (i) *p*-wave, (ii) *d*-wave, and (iii) *f*-wave have been considered. The calculation results suggest that we can clearly distinguish the present three pairing symmetries from tunneling spectroscopy. We believe our theoretical prediction can be verified experimentally in the near future. It is an interesting future problem to investigate how our results will be modified for $(\text{TMTSF})_2\text{ClO}_4$, in which a unit cell doubling due to anion ordering takes place.²⁷ It is also an interesting future problem to study Josephson effect in Q1D organic superconductors since it has been clarified in the previous studies that Josephson effect are crucially influenced by unconventional pair potentials.³¹

First author (Y. T.) acknowledges the financial support of Research Fellowships of Japan Society for the Promotion of Science (JPSJ) for Young Scientists. K.K. acknowledges Hideo Aoki for discussions and pointing out Ref. 27. The computational aspect of this work has been performed at the facilities of the Supercomputer Center, Institute for Solid State Physics, University of Tokyo and the Computer Center.

¹ D. J. Scalapino, Phys. Rep. **250**, 329 (1995).

² M. Sigrist and K. Ueda, Rev. Mod. Phys. **63**, 239 (1991).

³ S. Kashiwaya and Y. Tanaka, Rep. Prog. Phys. **63**, 1641 (2000).

⁴ D. Jerome, A. Mazaud, M. Ribault, and K. Bechgaard, J. Phys. Lett. (France) **41**, L92 (1980).

⁵ I.J. Lee, M.J. Naughton, G.M. Danner, and P.M. Chaikin, Phys. Rev. Lett. **78**, 3555 (1997); I.J. Lee, P.M. Chaikin, and M.J. Naughton, Phys. Rev. B **62**, R14 669 (2000).

⁶ I.J. Lee, D.S. Chow, W.G. Clark, J. Strouse, M.J. Naughton, P.M. Chaikin, and S.E. Brown, cond-mat/0001332.

⁷ M. Takigawa, H. Yasuoka, and G. Saito, J. Phys. Soc. Jpn. **56**, 873 (1987).

⁸ S. Belin and K. Behnia, Phys. Rev. Lett. **79**, 2125 (1997).

⁹ A.A. Abrikosov, J. Low Temp. Phys. **53**, 359 (1983).

¹⁰ Y. Hasegawa and H. Fukuyama, J. Phys. Soc. Jpn. **56**, 877 (1987).

¹¹ A.G. Lebed, Phys. Rev. B **59**, R721 (1999); A.G. Lebed, K. Machida, and M. Ozaki, Phys. Rev. B **62**, R795 (2000).

¹² R.L. Greene and E.M. Engler, Phys. Rev. Lett. **45**, 1587 (1980).

¹³ H. Shimahara, J. Phys. Soc. Jpn. **58**, 1735 (1989).

¹⁴ K. Kuroki and H. Aoki, Phys. Rev. B **60**, 3060 (1999).

¹⁵ H. Kino and H. Kontani, J. Low. Temp. Phys. **117**, 317 (1999).

¹⁶ J.P. Pouget and S. Ravy, J. Phys. I (France) **6**, 1501 (1996).

¹⁷ S. Kagoshima, Y. Saso, M. Maesato, R. Kondo, T. Hasegawa, Solid State Commun. **110**, 479 (1999).

¹⁸ K. Kuroki, R. Arita, and H. Aoki, cond-mat/0006218.

¹⁹ C.R. Hu, Phys. Rev. Lett. **72**, 1526 (1994).

²⁰ Y. Tanaka and S. Kashiwaya, Phys. Rev. Lett. **74**, 3451 (1995).

²¹ J. Geerk, X.X. Xi, and G. Linker, Z. Phys. B. **73**, 329 (1988).

²² L. Alff, H. Takashima, S. Kashiwaya, N. Terada, H. Ihara, Y. Tanaka, M. Koyanagi, and K. Kajimura, Phys. Rev. B **55**, 14757 (1997).

²³ J.Y.T. Wei, N.-C. Yeh, D.F. Garrigus, and M. Strasik, Phys. Rev. Lett. **81**, 2542 (1998).

²⁴ W. Wang, M. Yamazaki, K. Lee, and I. Iguchi, Phys. Rev. B **60**, 4272 (1999).

²⁵ K. Sengupta, I. Žutić, H.-J. Kwon, V.M. Yakovenko, and S. Das Sarma, cond-mat/0010206.

²⁶ Y. Tanuma, Y. Tanaka, M. Yamashiro, and S. Kashiwaya, Phys. Rev. B **58** 7997 (1997).

²⁷ H. Yoshino, A. Oda, T. Sasaki, T. Hanajiri, J. Yamada, S. Nakatsuji, H. Anzai, and K. Murata, J. Phys. Soc. Jpn. **68**, 3142 (1999).

²⁸ M. Tachiki, S. Takahashi, F. Steglich and H. Adrian, Z. Phys. B **80**, 161 (1990).

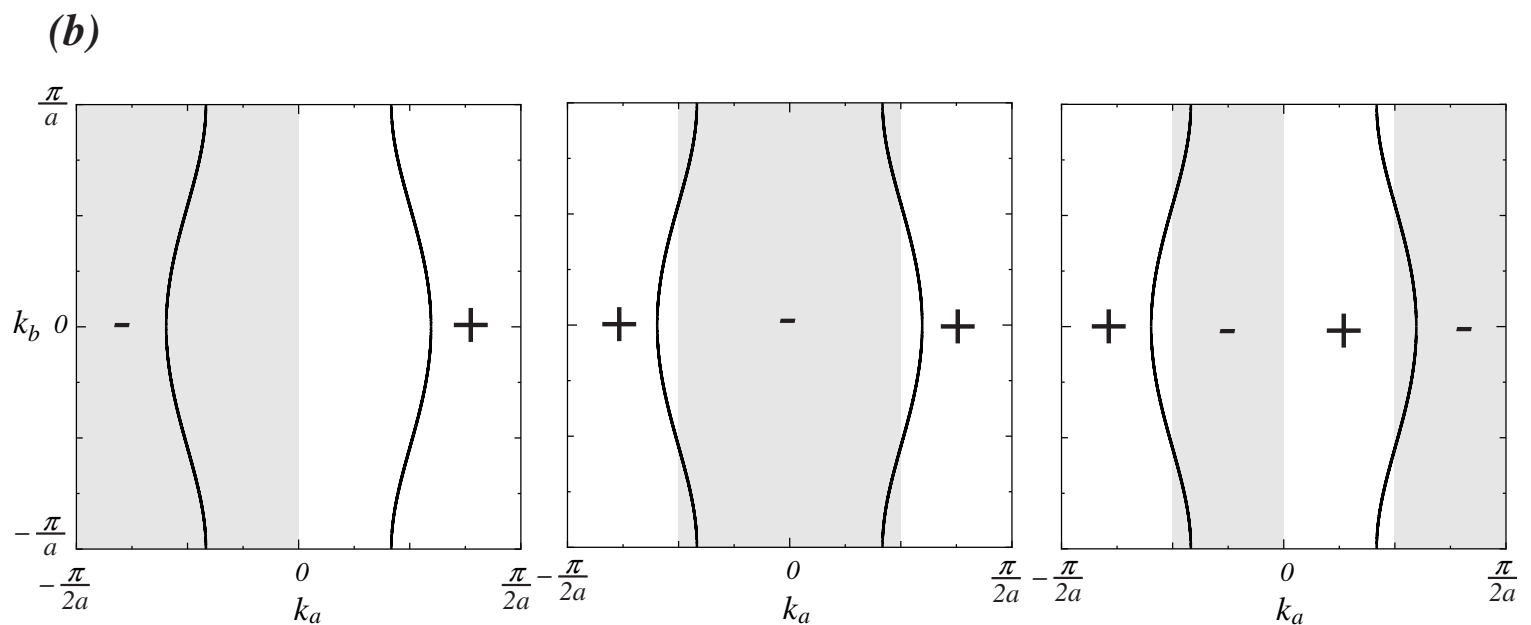
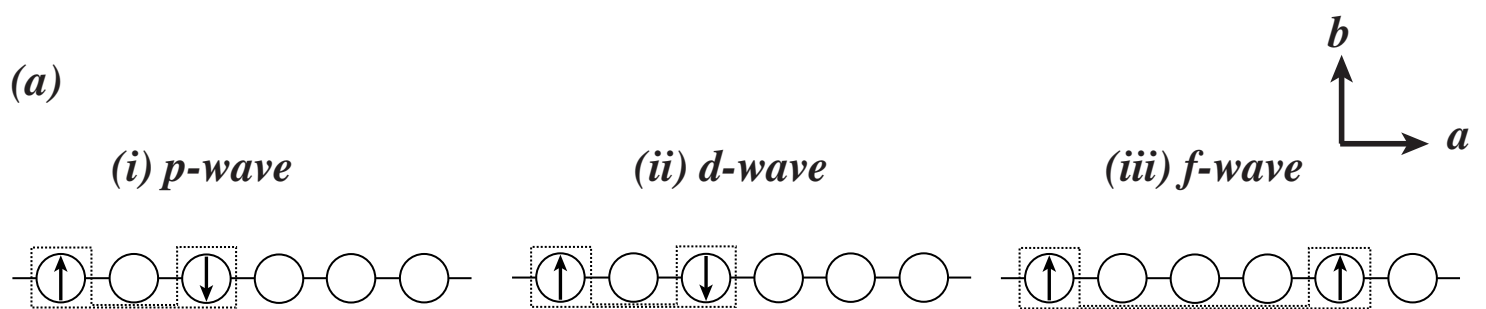
²⁹ M. Tinkham, *Introduction to Superconductivity* (McGraw-Hill, New York, 1975).

³⁰ L.J. Buchholtz and G. Zwicknagl, Phys. Rev. B **23**, 5788 (1981).

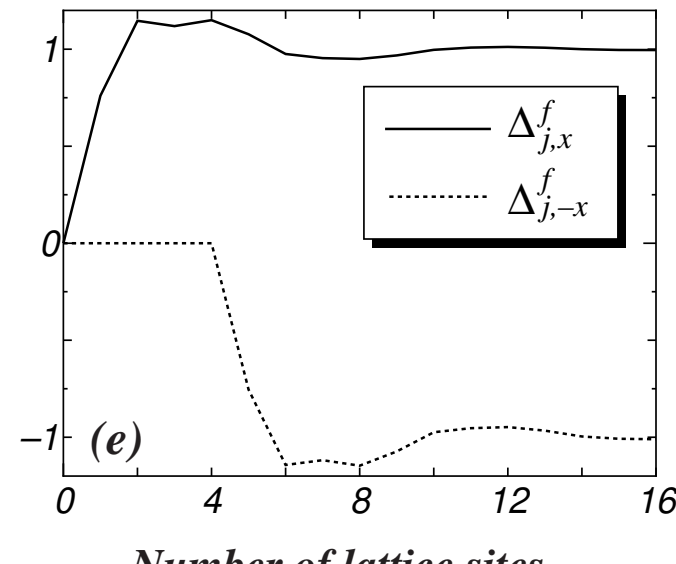
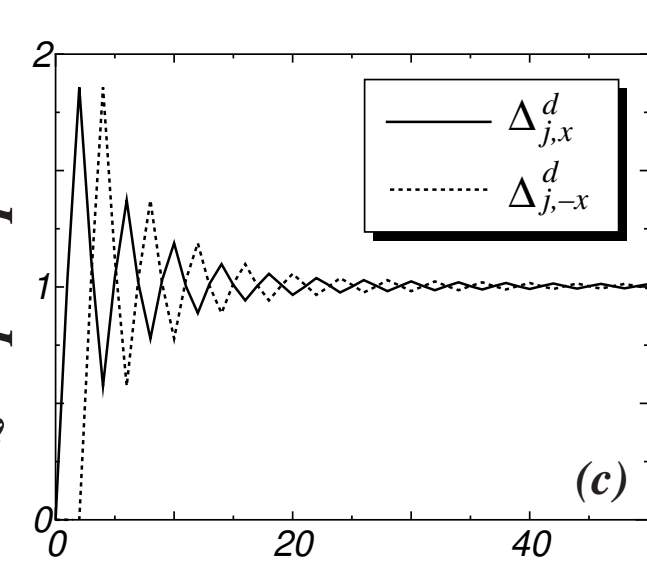
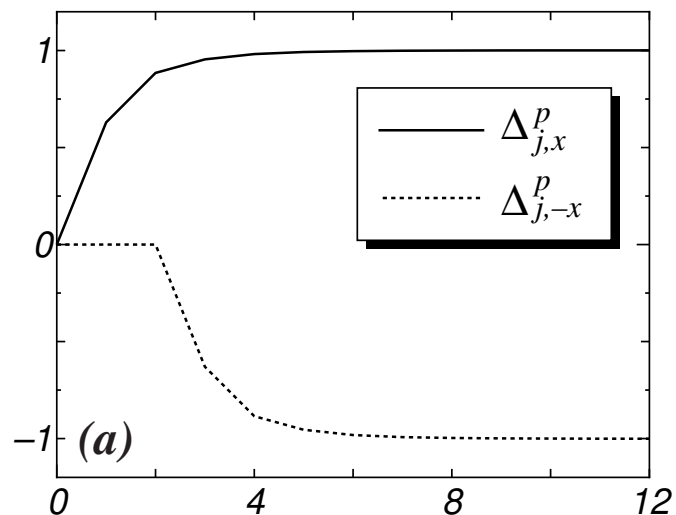
³¹ Y. Tanaka and S. Kashiwaya, Phys. Rev. B **53** 11957 (1996), Phys. Rev. B **56** 892 (1997).

TABLE I. Surface density of states (SDOS) for *p*, *d*, and *f*-wave pairings.

Symmetry	SDOS
<i>p</i> -wave	U-shaped + <i>a</i> -axis ZEP
<i>d</i> -wave	V-shaped + No ZEP
<i>f</i> -wave	V-shaped + <i>a</i> -axis ZEP



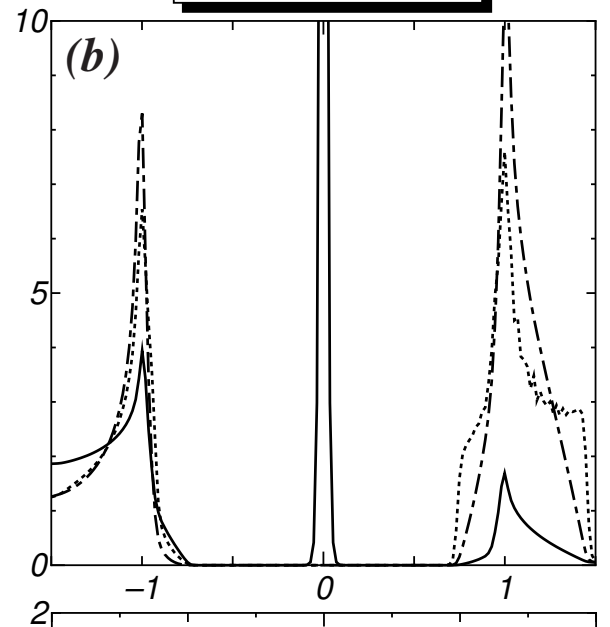
Normalized pair potential



a-axis ———

b-axis - - -

bulk - - - -



Normalized Local Density of States

